Available online at www.sciencedirect.com
ScienceDirect
Geochimica et Cosmochimica Acta 72 (2008) 1257–1268
Geochimica et Cosmochimica Acta
www.elsevier.com/locate/gca

Acid–base properties of cyanobacterial surfaces I: Influences of growth phase and nitrogen metabolism on cell surface reactivity

S.V. Lalonde [a,*], D.S. Smith [b], G.W. Owttrim [c], K.O. Konhauser [a]

[a] *Department of Earth and Atmospheric Sciences, University of Alberta, 3-13 Earth Science Building, Edmonton, AB, Canada T6G 2E3*
[b] *Department of Chemistry, Wilfrid Laurier University, Waterloo, ON, Canada N2L 3C5*
[c] *Department of Biological Sciences, University of Alberta, Edmonton, AB, Canada T6G 2E9*

Received 20 April 2007; accepted in revised form 1 October 2007

Abstract

Significant efforts have been made to elucidate the chemical properties of bacterial surfaces for the purposes of refining surface complexation models that can account for their metal sorptive behavior under diverse conditions. However, the influence of culturing conditions on surface chemical parameters that are modeled from the potentiometric titration of bacterial surfaces has received little regard. While culture age and metabolic pathway have been considered as factors potentially influencing cell surface reactivity, statistical treatments have been incomplete and variability has remained unconfirmed. In this study, we employ potentiometric titrations to evaluate variations in bacterial surface ligand distributions using live cells of the sheathless cyanobacterium *Anabaena* sp. strain PCC 7120, grown under a variety of batch culture conditions. We evaluate the ability for a single set of modeled parameters, describing acid–base surface properties averaged over all culture conditions tested, to accurately account for the ligand distributions modeled for each individual culture condition. In addition to considering growth phase, we assess the role of the various assimilatory nitrogen metabolisms available to this organism as potential determinants of surface reactivity. We observe statistically significant variability in site distribution between the majority of conditions assessed. By employing post hoc Tukey–Kramer analysis for all possible pair-wise condition comparisons, we conclude that the average parameters are inadequate for the accurate chemical description of this cyanobacterial surface. It was determined that for this Gram-negative bacterium in batch culture, ligand distributions were influenced to a greater extent by nitrogen assimilation pathway than by growth phase.

1. INTRODUCTION

The ubiquitous presence of bacteria in surface environments, along with their chemical reactivity, make them important factors in driving elemental cycling on the Earth's surface. In particular, organic functional groups located in the bacterial cell wall act as highly efficient ligands for the sorption of metals (e.g., Beveridge and Murray, 1980; Beveridge et al., 1982; Daughney and Fein, 1998; Daughney et al., 1998) and/or organic compounds (Baughman and Paris, 1981; Fein and Delea, 1999). Those ligands also determine the overall cell surface charge governing bacterial adherence to solid substrata (van Loosdrecht et al., 1989, 1990; Yee et al., 2000), which in turn, impacts on metal mobility in many fluid-rock systems (e.g., McCarthy and Zachara, 1989; Lindgvist and Enfield, 1992; Corapcioglu and Kim, 1995). The sorptive capacity of bacteria additionally alters mineral precipitation and dissolution rates at the bacterial surface (Konhauser et al., 1993; Fortin et al., 1997; Warren and Ferris, 1998).

Potentiometric titrations have been employed to determine discrete proton-exchanging surface ligands for an increasing number of bacterial strains (e.g., Plette et al., 1995; Fein et al., 1997; Cox et al., 1999; Haas et al., 2001, 2004; Sokolov et al., 2001; Martinez et al., 2002; Phoenix et al., 2002; Ngwenya et al., 2003; Yee et al., 2004; Borrok

* Corresponding author.
E-mail address: stefan.lalonde@ualberta.ca (S.V. Lalonde).

0016-7037/$ - see front matter
doi:10.1016/j.gca.2007.10.031

et al., 2004, 2005) using a diverse selection of modeling techniques (reviewed by Fein et al., 2005). While these may vary in mathematical approach and assumptions made regarding electrostatic phenomena at the bacterial surface, they are unified in their goal of providing parameters, such as ligand concentrations and proton–ligand stability constants, that quantitatively describe the bacterial surface. These modeled parameters are considered constants that, when applied to artificial or natural geochemical systems using a chemical surface complexation approach, successfully enable quantitative predictions of mass balance with respect to those surfaces under a variety of conditions (e.g., Fowle and Fein, 1999). Daughney et al. (2001) first pointed out that while surface complexation models may accurately account for the influence of abiotic variables on the bacterial metal adsorption process, biotic variables have been largely ignored. The bacterial surface is a highly dynamic interface where new cell wall material and/or extracellular layers are added, proteins are inserted, signals are transduced, adherence to solid substrata occurs, flocculation and motility are controlled, and nutrients and metabolites are exchanged.

Preliminary studies have begun to reveal biological processes affecting ligand distribution on Gram-positive (Daughney et al., 2001) and Gram-negative (Haas, 2004; Borrok et al., 2004) bacterial surfaces, and there exists some evidence indicating that for a single bacterial species, metal adsorption may be controlled by variations in ligand distributions that ultimately arise as a consequence of the diversity of conditions under which the bacteria may grow. Metal adsorption studies indicate an important role for proton-exchanging (i.e., carboxyl) ligands in metal sorption (Fein et al., 1997; Daughney et al., 1998; Fowle et al., 2000; Daughney et al., 2001), and variability in the concentration of some ligand-bearing organic components of the cell wall (i.e., techoic and teichuronic acids) has been shown to influence the metal sorption process (Beveridge and Murray, 1980; Beveridge et al., 1982). Efforts to reveal biological controls on the extent of metal sorption have focused largely on the life cycle of a laboratory batch culture; at high nutrient and/or low metabolite concentrations, cells proliferate exponentially to the point where growth is limited by the total consumption of one or more nutrients, or metabolites reach toxic levels, and cell populations remain stationary (Madigan et al., 1997).

Growth phase has been implicated as a factor in metal sorption for a variety of bacteria with mixed results (Friis and Meyers-Keith, 1986; Chang et al., 1997; Daughney et al., 2001), and it is likely that the effects of growth phase are species-specific (Daughney et al., 2001). For example, Daughney et al. (2001) indicated that such growth effects can be of sufficient significance as to affect the outcome of surface complexation models employing the Gram-positive *Bacillus subtilis*, while Haas (2004) concluded that growth phase had negligible influence on the ligand distributions of the Gram-negative *Shewanella putrefaciens*. Both Haas (2004) and Borrok et al. (2004) have further assessed the role of nutrient concentration on the surface reactivity of *S. putrefaciens* and *Pseudomonas fluorecens*, respectively, and they accepted the null hypothesis in this respect. As progression through growth phases is dictated in part by nutrient concentration, it is not surprising that any variability associated with growth phase might also include variability attributable to nutrient concentration.

The situation becomes more complex with the consideration of facultative metabolic pathways. For bacteria that are capable of switching between multiple metabolic pathways, the presence or absence of specific nutrients may dictate the expression of nutrient-specific chelation agents and membrane transport proteins (e.g., Wandersman and Delepelaire, 2004), the production of extracellular polymers (Rinker and Kelly, 2000), adhesion in biofilm communities (Thormann et al., 2005), and cellular differentiation such as heterocyst formation (see Wolk, 1996 for review). Both Haas (2004) and Borrok et al. (2004) considered facultative aerobic and anaerobic dissimilatory metabolism in their investigations, with mixed results. While Borrok et al. (2004) found that the metabolic pathway of growth had negligible effect on Co adsorption by *Shewanella oneidensis* MR-1, Haas (2004) found sufficient variability by potentiometric titration of *S. putrefaciens* as to warrant two distinct sets of surface parameters, each specific to a particular metabolic pathway, for the accurate description of this microbial surface. Hong and Brown (2006), evaluating the role of growth phase, nitrate vs. ammonium N sources, and media C:N ratio on the surface reactivity of *Escherichia coli* K-12 and *Bacillus brevis* found that only N source influenced the surface reactivity of the former, and only C:N ratio influenced the latter. Clearly, controversy remains regarding metabolic determinants of microbial surface reactivity, and facultative variation has only been assessed between microbes of the same genus and metabolic capability.

In this study, we consider the potential role that assimilatory metabolism may play in determining surface ligand distributions. Specifically, we evaluate:

(1) the acid–base properties of a well-characterized, unsheathed cyanobacterium (*Anabaena* sp. strain PCC 7120) in order to contribute to the collection of chemical parameters describing the surfaces of diverse bacteria,
(2) proton sorption by the same cyanobacterium grown under conditions ensuring assimilatory nitrate reduction, ammonium assimilation, and nitrogen fixation, with the goal of revealing variability in surface chemistry as a reflection of compositional differences in cell wall architecture as dictated by specific N availability,
(3) the role of growth phase, complimenting data previously reported for variability in the surface chemistry of a Gram-positive bacterium (Daughney et al., 2001) and Gram-negative bacteria (Haas, 2004; Borrok et al., 2004).

We report a set of average surface chemical parameters modeled from replicate potentiometric titrations of cells over two growth phases and three nitrogen metabolisms, and statistically evaluate the ability of the average parameters to account for the variations in surface chemical parameters observed between individual conditions.

2. METHODS

2.1. Growth procedures

The cyanobacterial strain *Anabaena* sp. PCC 7120 (henceforth referred to as *Anabaena*) was chosen for its lack of sheath or S-layer (Rippka et al., 1979), ability to fix atmospheric nitrogen via heterocyst formation, and well characterized genome (Kaneko et al., 2001). Axenic cultures were grown under constant illumination of ~100 microeinsteins/m^2/s in liquid BG-11 media (Rippka et al., 1979) at 30 °C with aeration provided by shaking at 150 rpm and bubbling with filtered and humidified air (Chamot and Owttrim, 2000). Separate populations consistently limited, over at least 3 transfers, to growth on either nitrate, ammonium, or dinitrogen as the sole nitrogen source were maintained in nitrogen-free BG-11(0) media to which 17.6 mM of nitrate as $NaNO_3$, 17.6 mM ammonium as NH_4Cl, or 17.6 mM NaCl (no fixed nitrogen source) was added, respectively. For *Anabaena* species, heterocyst formation, and therefore nitrogen fixation, is inhibited by the addition of a fixed nitrogen source (Wolk, 1996). For all media, the BG-11 ingredients containing fixed nitrogen (ferric ammonium citrate and cobaltous nitrate hexahydrate) were replaced with nitrogen-free equivalents (ferric citrate and cobaltous chloride hexahydrate), and the media was buffered around pH 8 by the addition of 10 mM Tricine.

The three cell populations were maintained as stock cultures by successive transfers into 50 ml of media with 10% v/v inoculations. In order to obtain sufficient biomass for potentiometric titration, 3 L cultures were established in 6 L Erlenmeyer flasks, magnetically stirred, and bubbled with filtered air. The 10% inoculum used to establish the large cultures was derived from 300 ml cultures prepared from, and supplementary to, the 50 ml stock cultures. Growth was monitored by optical density measurements at 595 nm, and cultures were harvested at an absorbance of 0.3 ± 0.03 (~0.13 g dry weight/L) for exponential phase cells, and 0.6 ± 0.03 (~0.24 g dry weight/L) for stationary phase cells. Although growth rate varied according to nitrogen assimilatory pathway, and therefore the time of harvest varied for each condition, differences in growth between conditions were largely associated with lag phase, the above absorbance values fell within exponential and stationary growth phases for all conditions.

Cells were harvested by centrifugation at room temperature (11,050*g*, 10 min) and prepared at pH ~ 7 by three washes with 200 ml of 18.2 MΩ water, followed by four washes with 50 ml of 0.01 M KNO_3 titration electrolyte. Between washes, the cells were incubated for 10 min, pelleted by centrifugation as above, and the supernatant discarded. After the last wash, the concentrated biomass deriving from 1 L of culture was suspended in 0.01 M KNO_3 to a final volume of 50 ml.

2.2. Potentiometric titrations

All plastic and glassware used for solution preparation and potentiometric titration were soaked in 10% v/v nitric acid for 24 h and subsequently in 18 MΩ sterile water for 48 hours (Cox et al., 1999). All solutions were prepared according to standard analytical methods (Harris, 1995) using sterile 18 MΩ water purged of dissolved CO_2 with N_2(g) for at least 30 minutes and stored under a nitrogen atmosphere. The 0.01 M KNO_3 titration electrolyte was prepared volumetrically by the addition of weighed KNO_3 salt, and 0.2 M HNO_3 as well as 0.01 M NaOH were similarly prepared using 50% NaOH solution and concentrated trace-metal nitric acid, respectively. Solutions were standardized by titration against dried potassium hydrogen phthalate prior to titration according to the methodology of Cox et al. (1999).

Before each titration, 10 g of concentrated (2.6–4.8 g dry weight/L) biomass suspension was added to 40 g of KNO_3 electrolyte solution in a titration flask prefitted with a Ross-type glass pH electrode (Man-Tech Associates Inc., Guelph, ON), reduced to pH ~3.2 with 200 µl 0.2 M HNO_3, and allowed to equilibrate for 30 min under a constant purge of N_2 gas. Titrations were performed alkalimetrically from pH ~ 3.2 to pH 11 using a QC-Titrate autotitrator (Man-Tech Associates Inc., Guelph, Ontario) variably delivering CO_2-free 0.01 M NaOH for 0.1 pH increments and maintaining electrode stability criteria of <1 mV/s. The average equilibration time between additions was ~30 s. The system was continuously purged with N_2 gas and magnetically stirred. The pH electrode was calibrated using commercial buffers, and assessed for drift between titrations using the same buffers. A thermocouple was used to compensate pH calibration as well as verify that temperature remained within 1 degree of 23 °C throughout titration.

Immediately following titration, biomass was filtered onto preweighed Whatman GF/C #42 filters (Whatman Inc., Florham park, New Jersey) and oven dried at 70 °C for 48 h prior to weighing. Each condition tested was represented by one liter of culture that yielded concentrated biomass for 5 replicate and consecutive titrations. The exponential and stationary phase biomass for titration was harvested at different times from the same 3 L culture, for each nitrogen metabolism. Heat-killed biomass was similarly harvested as stationary phase biomass, but autoclaved at 121 °C for 20 min after the final resuspension in KNO_3 electrolyte, and titrated upon cooling. All titrations were performed within 18 h of biomass harvesting, and cellular integrity was assessed before and after titration by pigment autofluorescence using a Zeiss Axioskop 2 epi-fluorescent light microscope; any cells that have lysed may appear intact, but do not display autofluorescence. No change in the relative abundance of cells that displayed autofluorescence was noted after the titration procedure.

2.3. Modeling of ligand concentrations

Bacterial ligand concentrations and acid-neutralizing capacity were fit to the titration data using a pK_a spectrum approach; pK_a values were fixed in a chosen interval (in this case, 3–11 in intervals of 0.2) and ligand concentrations at each pK_a value were fit using a linear-programming approach (Brassard et al., 1990; Smith and Kramer, 1999; Smith et al., 1999; Cox et al., 1999; Martinez and Ferris,

2001; Martinez et al., 2002; Phoenix et al., 2002; Fein et al., 2005). By fixing the possible pK_a values and then optimizing the ligand concentrations for each possible pK_a value, the number of distinct sites of significant concentration are not fixed, but rather are returned from the fitting procedure. The linear-programming method determines by iteration the ligand concentrations that minimize the absolute of the error between the charge excess measured by titration and the charge excess resulting from the iteratively proposed ligand concentrations. In order to calculate charge excess, the charge balance of the system is first expressed as:

$$C_b + [H^+] + [ANC] = C_a + [OH^-] + \sum_{j=1}^{n} [L_j^-] \quad (1)$$

where C_b and C_a are the concentrations of base and acid, respectively, $[H^+]$ and $[OH^-]$ are measured by the pH electrode, $[L_j^-]$ is the concentration of deprotonated functional groups for the jth monoprotic site of n possible sites set by the pK_a spectrum, and the acid-neutralizing capacity [ANC] is a constant representing the difference between functional groups that remain protonated and those that remain deprotonated over the titration range (Smith and Ferris, 2001). Blank titrations were performed to confirm that the electrolyte solution and experimental error contributed negligibly to charge excess over the modeled pH range. Charge excess due to experimental error (discussed below) became important below pH ~3.5 and above pH ~10.4.

The charge balance can be rewritten such that, for the ith addition of titrant, charge excess $b_{i\ \mathrm{fit}}$ represents the contribution of bacterial functional groups to the charge balance as fit by linear programming. Similarly, this rearrangement allows for $b_{i\ \mathrm{measured}}$ to be assessed in terms of measured parameters:

$$b_{i\ \mathrm{fit}} = \sum_{j=1}^{n} [L_j^-] - [ANC] \quad (2)$$

$$b_{i\ \mathrm{measured}} = C_{b_i} - C_{a_i} + [H^+]_i - [OH^-]_i \quad (3)$$

The set of ligand concentrations that best fit the titration data is obtained when $b_{i\ \mathrm{fit}}$ approaches $b_{i\ \mathrm{measured}}$. The ANC term is recovered by modeling, and serves as a constant offset for b_{fit}, and thus does not represent total buffering capacity in the tradition sense of the word. This method assumes a value of zero for $b_{i\ \mathrm{measured}}$ at the pH of the suspension prior to acidification, although this value may be considered arbitrary and is accounted for in the ANC term. As such, inferences regarding absolute surface charge of the bacterial surface is not possible by this method; discussion of absolute surface charge is avoided, in part because it has been shown that bacteria may continue to adsorb protons and metals at pH values well below the titration range reported here (Fein et al., 2005).

For the jth site with a value of K_{aj} provided by the chosen pK_a spectrum, at the ith addition of titrant, the deprotonated site concentration $[L_j^-]$ is related to the total site concentration $[L_{Tj}]$ by the expression:

$$[L_j^-] = \frac{K_{aj}[L_{Tj}]}{[H^+]_i + K_{aj}} \quad (4)$$

After fixing the possible pK_a values using the spectrum approach, $[L_{Tj}]$ and [ANC] are readily fit to the measured excess charge $b_{i\ \mathrm{measured}}$. The linear-programming method iteratively calculates the charge excess deriving from a proposed set of positive ligand concentrations ($b_{i\ \mathrm{fit}}$) as:

$$b_{i\ \mathrm{fit}} = \sum_{j=1}^{n} \frac{K_{aj}[L_{Tj}]}{[H^+]_i + K_{aj}} - [ANC] \quad (5)$$

and fits the data by minimizing the difference between $b_{i\ \mathrm{measured}}$ and the $b_{i\ \mathrm{fit}}$ using the simplex algorithm. This method emphasizes zero as a possible solution and minimizes the number of sites that are required to describe the data. All pK_a values reported here are apparent; electrostatic potential corrections are not applied, although the results are likely comparable with other studies that employ electrostatic models, as it has been suggested that bacterial surface electric field effects are negligible for proton adsorption (Borrok et al., 2004; Borrok and Fein, 2005). Non-electrostatic and electrostatic models describing the bacterial surface have been recently compared by Borrok and Fein (2005), and it was demonstrated that electrostatic models, originally developed to describe mineral surfaces, overemphasize the role of electrical potential in determining bacteria-solute interactions. In the same study, proton adsorption was best described for two Gram-negative bacteria by a non-electrostatic model (Borrok and Fein, 2005).

3. RESULTS AND DISCUSSION

3.1. Charge excess data

In order to assess the variance of model parameters using replicates of a single condition, each individual titration was modeled and plotted independently. The measured and fitted charge excess curves for live cultures are plotted as a function of growth phase and nitrogen metabolism in Fig. 1. On the charge excess curves, the slope at any given point corresponds to the buffer capacity at the point. In other words, the slope indicates the rate of ligand deprotonation, per unit of pH, at that point.

It is immediately evident from Fig. 1 that rapid changes in charge excess occurred at extreme pH values in all cases, suggesting the presence of significant concentrations of ligands with dissociation constants that lie outside of the titration range. Careful consideration of the system behavior and model limitations is required to fully explain the relevance of these hypothesized ligands to the model parameters reported below. Titrations were performed over a pH range of ~3.2 to 11 and modeled using data from pH 4 to 10, as uncertainty in measured charge excess increases at pH extremes due a combination of uncertainty in electrode calibration, increased possibility of cell lysis and/or release of organic exudates, and the decreasing importance of bacterial ligands in the charge balance expression (Smith et al., 1999). Furthermore, titrations were reversible over the pH 4–10 range, however hysteresis was apparent over the pH ~3.2 to 4 range (data not shown), possibly due to factors listed above. Using data from pH 4 to 10, ligand concentrations were then fit to a pK_a spectrum spanning from 3 to 11, in order to allow for any ligands with pK_a val-

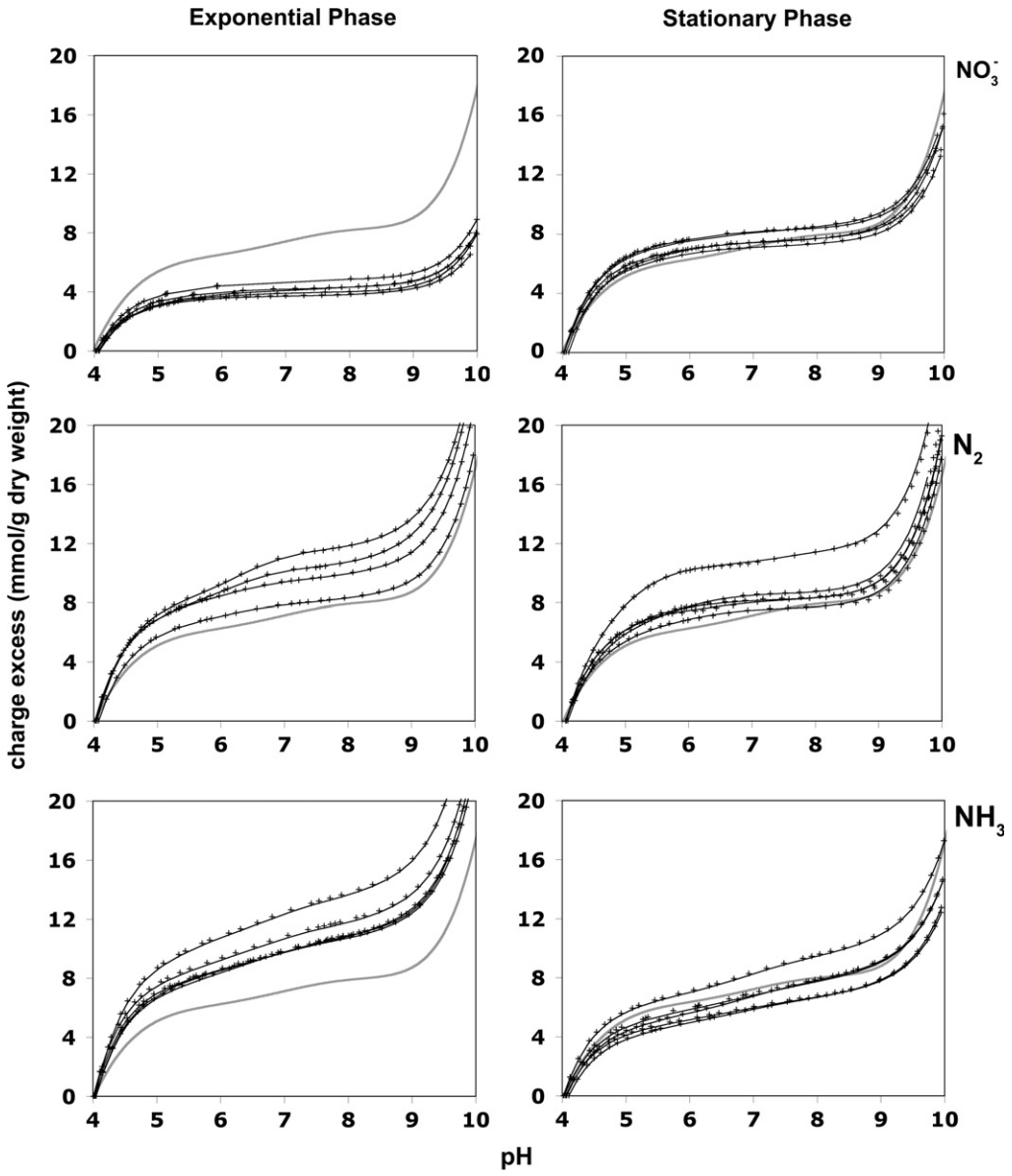

Fig. 1. Charge excess curves grouped as a function of growth phase and nitrogen metabolism. For each condition, all replicates are plotted, ($n = 5$, except for N_2 exponential phase, where $n = 4$) as well as the average of all titrations (grey line). In each plot, data points represent charge excess as measured by titration and smooth curves represent charge excess fitted by the corresponding ligand distribution models.

ues outside of the 4–10 data range to still affect the charge excess curve within the selected data range. Without this approach, the model attempts to assign large ligand concentrations to the upper and lower limits of the pK_a spectrum, but the resultant fit is poor in the pH 10–8.5 and 5.5–4 ranges as a set of ligands with pK_a values residing completely within the 4–10 range cannot adequately account for the charge excess behavior observed at the edges of the data range. The selection of titration data between pH 4 and 10 minimized the absolute error of the fitted charge excess while having a negligible effect on the concentrations and pK_a distributions of ligands with pK_a values between 4 and 10 (data not shown); in the case of this non-electrostatic model, less than 10% of ligands remain protonated at 1 pH unit from their equivalence point, and this drops below 1% at 2 pH units. It follows that ligands with pK_a values that fall outside of the selected range (4–10) will remain either largely protonated or largely deprotonated under most natural conditions. While this does not negate their importance in the interpretation of the charge excess data, it does mean that their availability as a site for metal adsorption is unlikely to vary over the circumneutral pH ranges typical of natural waters.

Sources of error inherent to the preparation procedure might incur effects that are manifested in the charge excess graphs. Despite the fact that the ionic strength of the BG-11 media (0.033 M in all cases) and the ionic strength of the titration electrolyte (0.01 M) were similar, the cells might have experienced some degree of osmotic shock during initial washes that employed deionized water (see above). The

possibility of pH shock during preparation was reduced by using solutions of circumneutral pH, close to the pH of the growth media. Epifluorescent microscopy confirming cell integrity by post-titration autofluorescence of cyanobacterial pigments indicates that any osmotic or pH shock experienced throughout the preparation and titration procedure did not lead to cell lysis, as the number of cells lacking photoactive pigments was negligible. However, titration suspensions were not assessed for organic or inorganic exudates post-titration, and their presence remains a possibility considering that K, Mg, Ca, dissolved organic carbon, proteins, and lipopolysaccharides can be released into solution following the prolonged immersion of bacterial cells in pH 10 electrolyte (Claessens et al., 2004). It follows that such cellular exudates may have contributed to the increased buffering observed at extreme pH (Fig. 1, discussed above). We present the charge excess curves (Fig. 1) for qualitative assessment of condition-specific charging profile and replicate repeatability only.

3.2. Discrete site modeling

The modeled parameters for all conditions investigated in this study are presented in Table 1. Also included in Table 1 are parameters previously reported for titrations of *Shewanella putrefaciens* (Haas, 2004), grown by aerobic and anaerobic metabolic pathways. It is evident that the values between these two Gram-negative bacteria are in close agreement, despite different preparation and titration methods, and that variability in ligand concentrations between *Anabaena* growth conditions exceeds that observed for *Shewanella putrefaciens*. Also included in Table 1 is data pertaining to heat-killed cell suspensions, discussed below.

For the purposes of statistical comparison, ligands were grouped according to broad pK_a ranges (4–7 and 7–10). This proved necessary due to the heterogeneity in the pK_a distribution of individual ligands between conditions; variation between conditions was sufficient to preclude the confident assignment of ligands that were equivalent between conditions. While statistical comparisons based on the two broad groupings eliminates the power to resolve differences on a ligand-by-ligand basis, it also greatly reduces the chance of type I statistical errors and increases the chance of type II errors. In other words, it decreases the chance of incorrectly finding statistical significance, and increases that chance of incorrectly rejecting statistical significance. Conclusions of difference based on these groupings are more robust by the conservative nature of this statistical approach.

Composite plots for each condition are presented in Fig. 2. In order to account for the number of occurrences of each ligand across replicates of a single condition, the composite plots were generated by summing the concentration of sites inferred for all replicates at each pK_a interval, and then dividing by the total sum of the biomass titrated over all replicates for that condition. In this manner, the composite plots present site concentrations that are weighted by their occurrence across all 5 replicates (with the exception of N_2 exponential phase, where $n = 4$).

It is apparent from Fig. 2 that there exists variation across conditions in the modeled number of sites, their concentrations, pK_a distributions, and in the variance between replicates. In all cases, at least three sites were required to describe the titration data, and given the range of pK_a values observed, a variety of functional groups may be ascribed to the results. As functional group classification cannot be wholly confirmed without additional (i.e., spectroscopic) evidence, a classification scheme will not be outlined here; we consider the pK_a classifications of Cox et al. (1999) as sufficient for the purposes of discussion.

Irrespective of growth phase, cultures grown by ammonium (NH_4^+) assimilation and by nitrogen fixation showed similar total ligand concentrations in the range of 3–4.5 mmol/g (Table 1), while those cultures grown on nitrate yielded concentrations approximately 50% lower. With respect to growth phase, those grown on ammonium or by nitrogen fixation both showed a decrease in total ligand concentrations in stationary phase relative to exponential phase cells, while nitrate (NO_3^-) grown cultures display the opposite trend. The former case is in concurrence with findings by Daughney et al. (2001), who found that the concentration of proton-exchanging ligands on the surface of

Table 1
Modeled site concentrations (in mmol per dry g) and pK_a distributions for all conditions investigated

pK_a class	4–7	7–10	Ratio (acidic to basic)	Total
NO_3 exp.	0.63 ± 0.08	0.06 ± 0.04	9.99	0.69 ± 0.07
NO_3 stat.	1.24 ± 0.08	0.30 ± 0.05	4.11	1.55 ± 0.10
N_2 exp.	2.75 ± 0.40	0.82 ± 0.15	3.35	3.57 ± 0.54
N_2 stat.	2.85 ± 0.49	0.18 ± 0.18	16.19	3.02 ± 0.65
NH_4^+ exp.	3.34 ± 0.18	1.06 ± 0.13	3.25	4.44 ± 0.25
NH_4^+stat.	2.18 ± 0.23	1.70 ± 0.10	1.28	3.88 ± 0.31
Average[a]	2.15 ± 0.24	0.68 ± 0.08	3.15	2.84 ± 0.45
S. putrefaciens Aerobic (Haas, 2004)[b]	0.99	0.79	1.24	1.78
S. putrefaciens Anaerobic (Haas, 2004)[b]	0.55	0.15	3.63	0.70
NO_3 heat-killed	3.18 ± 0.07	0.92 ± 0.04	3.46	4.10 ± 0.09
N_2 heat-killed	12.31 ± 0.67	6.39 ± 0.58	1.93	18.70 ± 0.59
NH_4 heat-killed	6.02 ± 1.13	7.67 ± 0.89	0.78	13.69 ± 1.01

Values are the average of five independently modeled titrations. Uncertainties are 1 standard error of the mean, where available.
[a] Values are the average of parameters modeled for all 29 live titrations ($n = 5$ except for "N_2 exp.", where $n = 4$).
[b] A wet to dry weight ratio of 10:1 was assumed.

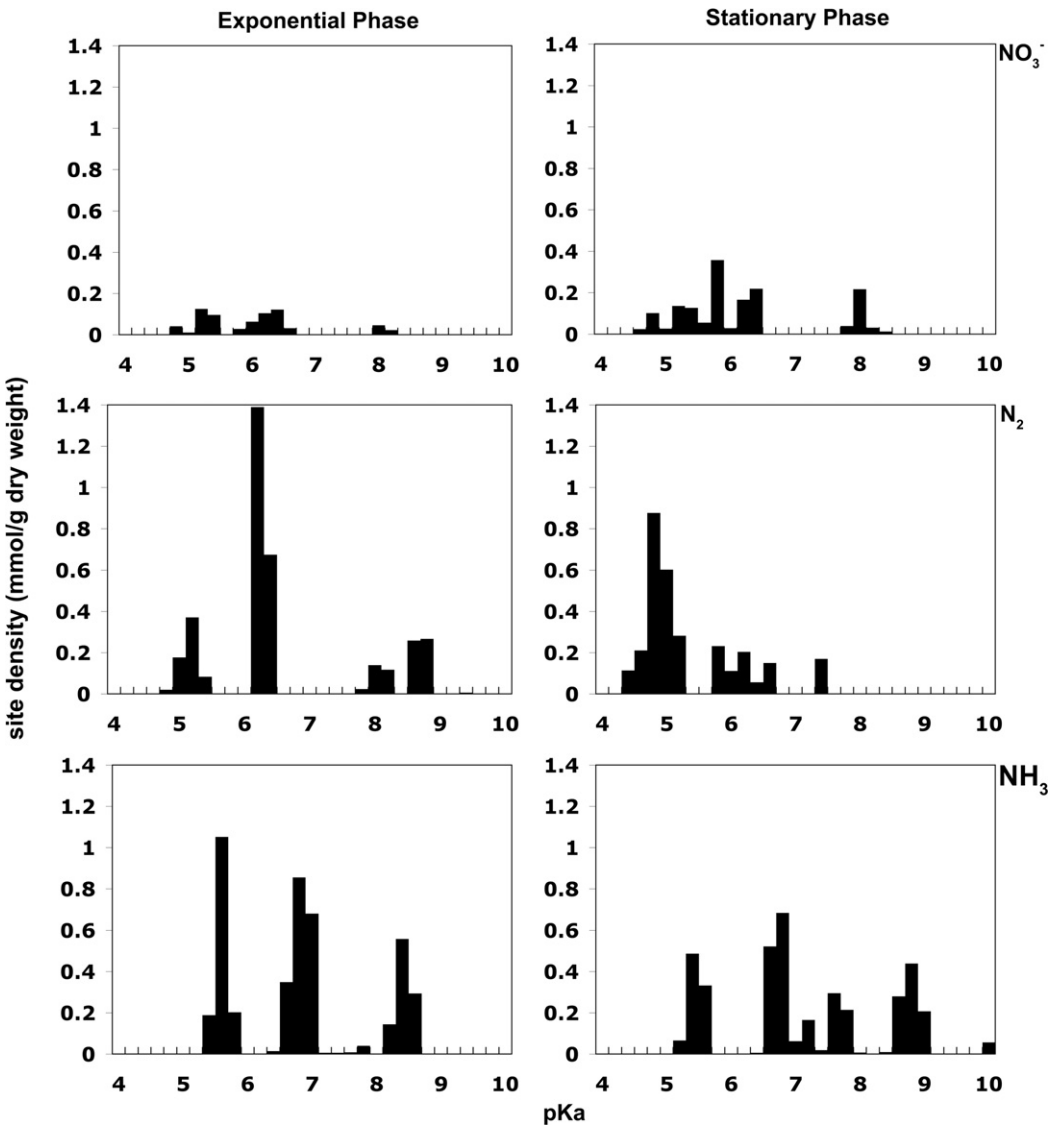

Fig. 2. Modeled ligand distributions grouped as a function of growth phase and nitrogen metabolism. Each panel accounts for all replicate titrations, with ligand concentrations weighted by occurrence at each pK_a interval (see text).

B. subtilis decreased from exponential to stationary phase. Previous studies of bacterial metal sorption (see introduction) have likewise indicated changes in surface chemistry between growth phases. As the surfaces of *Anabaena* and *B. subtilis* possess distinctly different architecture (Gram-negative vs. Gram-positive), the concurrence must be either coincidental, or the result of microbial success strategy that for unknown reasons has been selected for across distant positions, and between varying surface chemistries, within the bacterial domain. Similar trends were observed by Haas (2004) for *Shewanella putrefaciens*, who invoked changes in cell size to explain decreases on a per weight basis, and proposed that site concentrations increased on a per cell basis as a result of reserve polymer production and the expression of nutrient acquisition proteins. The filamentous nature of *Anabaena* prevented evaluation of our results on a per cell basis. It is possible that ligand concentrations are increased for exponential phase cells to facilitate the rapid acquisition of nutrients, and decreased for stationary phase cells to minimize interactions with toxic metabolites, or by the fact that the cells are no longer as metabolically active. It is equally possible, however, that an overall decrease in ligand concentrations may be detrimental at stationary phase by promoting interaction with toxic organic compounds and increasing the permeability of metal compounds that are no longer sequestered at the cell wall by reactive functional groups. Further experiments comparing the tolerance of exponential phase and stationary phase cells to increasing concentrations of toxins are necessary to determine the actual role, if any, of surface charge on metabolite or containment toxicity.

All conditions showed a greater concentration of ligands with pK_a values in the 4–7 range than in the 7–10 range, with an average acidic to basic ligand ratio of 3.15. Individ-

ual ligand pK_a values (and presumably, site identity) appear affected less by growth phase than by growth condition; hence, it would seem that growth conditions dictate the types of ligands expressed, while growth phase affects their relative concentrations. In order to determine the ability of one set of modeled parameters to describe all of the conditions with confidence, as well as distinguish trends that are statistically significant, one-way ANOVA as well as Tukey's post hoc comparisons were performed using the modeled parameters, as described below.

3.3. Titrations of heat-killed cell suspensions

Heat-killed cell suspensions were prepared with the intent of releasing all cytoplasmic contents, as well as fully exposing membranes, for characterization by titration, in order to determine whether the differences in reactivity attributed here to growth conditions might be reflected in cytoplasmic contents (i.e., in the intracellular pools of organic and inorganic compounds). Cell suspensions, prepared with concentrations of biomass equivalent to stationary phase titrations, were autoclaved for 20 min at 121 °C after the harvesting and washing procedure, and titrated upon cooling to room temperature. It should be noted that no attempt was made to separate cell membrane material from the cellular lysates; biomass was not washed after autoclaving, in order to retain soluble cytosolic contents and evaluate the biomass as a whole for compositional differences attributable to metabolic pathway. In turn, the heat-killed preparations likely differ significantly in terms of factors such as surface area, relative to the other titrations presented, and soluble biomass components likely contribute excess charge during these titrations. As a result, the numerical data from the heat-killed titrations has little relevance to modeling efforts beyond testing whether microbial biomass undergoes changes in acid–base behavior as the result of different growth conditions (which is the purpose of this study). Plots of excess charge and composite ligand profiles, categorized by growth condition, are presented in Fig. 3.

Excess charge curves (Fig. 3) clearly show that the cellular lysates provide considerably increased buffering capacity relative to intact cells. This is to be expected as many cytoplasmic contents, including both organic (e.g., cytosolic proteins, carbohydrates, nucleic acids) and inorganic (e.g., intracellular NH_4^+ and HCO_3^-) components, possess functional groups that deprotonate over the titration range. A twofold increase in buffering capacity might be expected from exposure of the cytoplasmic membrane's inner leaflet alone.

Overall, modeled total site densities were increased 2- to 6-fold by the sterilization process (Table 2). Composite plots (Fig. 3) reveal that the number of peaks invoked to fit the charge excess curves is increased relative to live cells, concordant with an increased diversity of exposed compounds. Again, cells grown by assimilatory nitrate reduction displayed overall ligand concentrations that were significantly (3–4 times) lower than those grown on other nitrogen sources. Such an important difference is difficult to reconcile; variation in the intracellular pools of organic compounds may be partially responsible. For example, the cyanobacterium *Synechocystis* sp. strain PCC6803 has been shown to increase intracellular glutamine concentrations by 30- to 40-fold within seconds of exposure to ammonium, although levels return to normal within ~30 minutes (Mérida et al., 1991). Variations in inorganic nitrogen pools (as a consequence of nitrogen metabolism) are unlikely to account for the observed results; in the case of the marine cyanobacterium *Synechococcus subsalsus*, non-protein-associated nitrogen constitutes less than 1% of total cellular nitrogen (Lourenço et al., 2004). This also implies that the reduced ligand concentrations inferred for the live nitrate-reducing cultures are a byproduct of cell wall compositional changes associated with growth by that metabolism. Interestingly, the most important ligands postulated for stationary phase cells grown by nitrogen fixation and ammonium assimilation are also most prominent for their heat-killed counterparts.

3.4. Statistical significance

In order to quantitatively assess the ability for the average modeled parameters (Table 1) to describe each condition investigated herein, statistical evaluations of confidence were performed in a pair-wise manner using the Tukey–Kramer test, a variant of the Tukey HSD (Honestly Significant Difference) test (Hsu, 1996). The Tukey–Kramer test is a post-hoc comparison used to supplement one-way ANOVA and provide pair-wise measures of confidence between means of different group sizes while controlling the rate of type I statistical error. For the pair-wise comparison of a large number of means, this is necessary as the probability of making a type I error (incorrectly assigning statistical significance) increases significantly with an increasing number of comparisons. For example, Daughney et al. (2001) performed 30 pair-wise comparisons based on 6 modeled parameters and 5 pairs using independent pair-wise one-way ANOVA. By this method, comparisons are independent of each other, and although the probability of incorrectly assigning significance is 0.05 for each comparison, the large number of individual comparisons increases the probability of incorrectly assigning significance at least once to over 50%. Haas (2004) performed multiple pair-wise comparisons using the Student's *t*-test, which similarly suffers from a type I error rate that increases with the number of comparisons made. While the increased possibility of a single type I error is perhaps insignificant to the findings of the aforementioned and otherwise well-executed studies, it can be avoided in future studies reporting multiple pair-wise comparisons. Tukey's HSD test enables this by employing a variation of the t distribution that accounts for the number of means being compared (the studentized range distribution) and maintains the overall type I error rate, rather than the individual comparison type I error rate, at the desired level of significance (0.05 in this case). The Tukey–Kramer test employs corrections for unequal replicate sizes, as the average parameters were determined from all 29 titrations and compared with conditions represented by 5 replicates (except N_2 exponential phase, where $n = 4$). One major assumption of this test

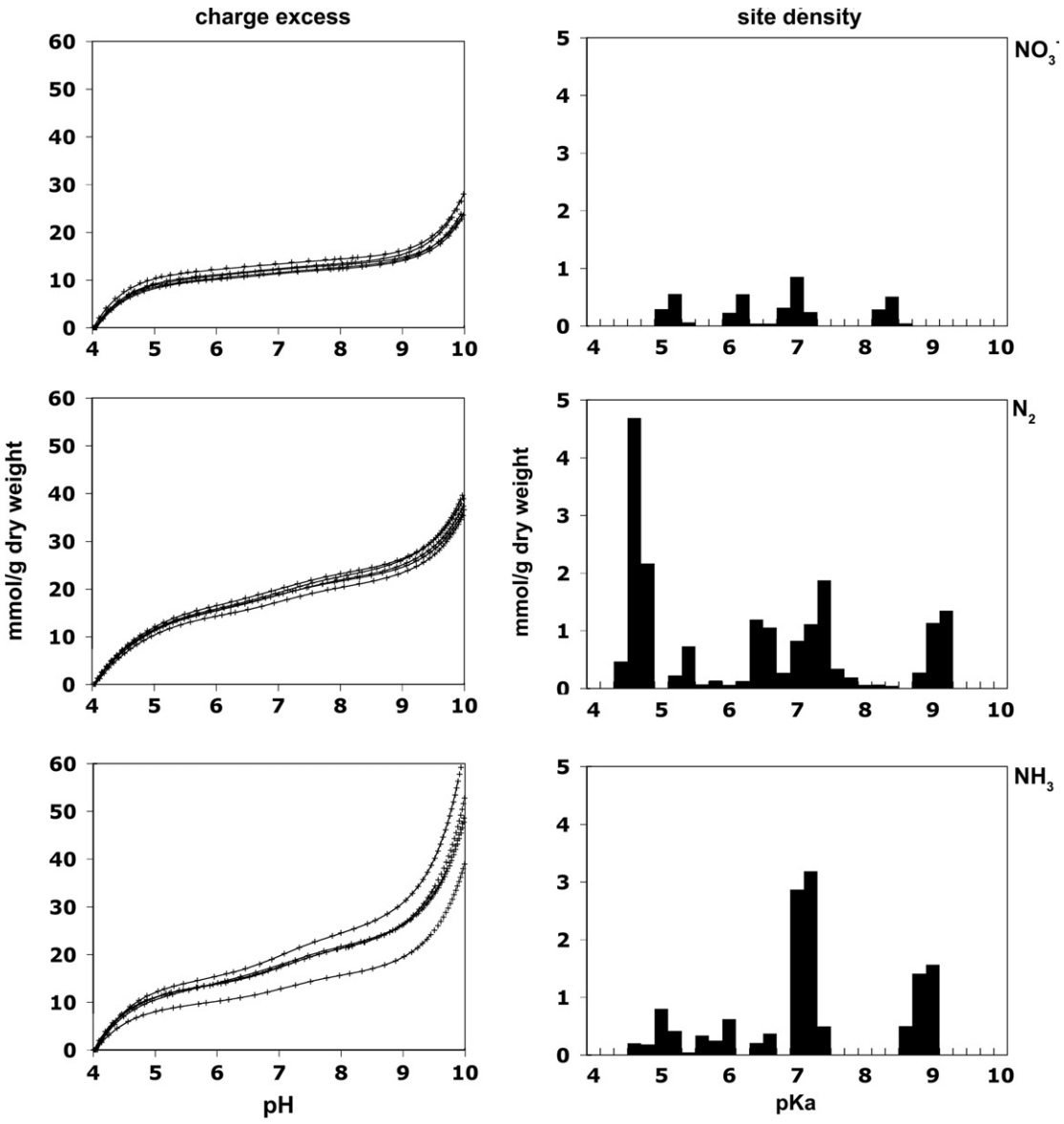

Fig. 3. Plots of charge excess and corresponding modeled ligand distributions for stationary phase cells lysed by autoclaving. For each condition, five replicates titrations are plotted. Data points represent charge excess as measured by titration and smooth curves represent charge excess fitted by the corresponding ligand distribution models. Modeled ligand distributions are composited over five replicate titrations for each condition, where ligand concentrations are weighted by occurrence at each pK_a interval (see text).

is that of equal variance between conditions, even though the apparent group variances are summed in the calculation of the mean squared error.

Two-tailed confidence intervals for all pair-wise comparisons are presented in Table 2. As mentioned above, the classification of ligands into broad groups rather than treatment on an individual basis serves to increase the importance of any variability that is deemed to be statistically significant. Confidence intervals greater than 0.95 indicate statistically significant similarity, while confidence intervals less than 0.05 indicate statistically significant difference. From Table 2, it is clearly apparent that the average model parameters are unable to describe the majority of conditions with confidence; in fact, with regards to total ligand concentration, the average parameters only describe stationary phase nitrogen fixing cells with confidence greater than 95%. Exponential nitrate-reducing and ammonium-assimilating cultures reject the average parameters with greater than 95% confidence, and the remainder are described with varying degrees of confidence. The situation is similar for comparison within ligand classes, with the average parameters providing weak support for the majority of conditions. These findings do not indicate that other investigations providing parameters describing bacterial surfaces are incorrect, but rather that previously reported parameters are likely to some degree dependent on culturing conditions. Due to large differences in architecture between the surfaces of Gram-positive and Gram-negative bacteria, the variability reported here for the surface of a Gram-negative bacterium does not likely extrapolate to

Table 2
Intervals of confidence in multiple pair-wise comparisons of ligand concentration as evaluated by Tukey post-hoc analysis (two-tailed p, $n = 7$, df = 52)

	Condition	NO_3 exp.	NO_3 stat.	N_2 exp.	N_2 stat.	NH_4 exp.	NH_4 stat.
Ligands with pK_a values 4–7	NO_3 exp.						
	NO_3 stat.	0.85					
	N_2 exp.	0.00	0.04				
	N_2 stat.	0.00	0.02	1.00			
	NH_4^+ exp.	0.00	0.00	0.87	0.94		
	NH_4^+stat.	0.03	0.44	0.88	0.79	0.19	
	Average	0.00	0.19	0.65	0.48	0.03	1.00
Ligands with pK_a values 7–10	NO_3 exp.						
	NO_3 stat.	0.92					
	N_2 exp.	0.02	0.23				
	N_2 stat.	1.00	1.00	0.07			
	NH_4^+ exp.	0.00	0.02	0.93	0.00		
	NH_4^+stat.	0.00	0.00	0.00	0.00	0.07	
	Average	0.01	1.00	0.98	0.06	0.29	0.00
All ligands	NO_3 exp.						
	NO_3 stat.	0.82					
	N_2 exp.	0.00	0.04				
	N_2 stat.	0.01	0.25	0.98			
	NH_4^+ exp.	0.00	0.00	0.81	0.27		
	NH_4^+stat.	0.00	0.01	1.00	0.82	0.97	
	Average	0.00	0.14	0.75	1.00	0.03	0.36

Gram-positive bacterial surfaces. Additional investigation using Gram-positive bacteria, employing diversity in both dissimilatory and assimilatory metabolic pathways, is required to fully assess the variability of that surface type. From these results, it appears that future characterizations of Gram-negative surface chemistry should attempt to as-

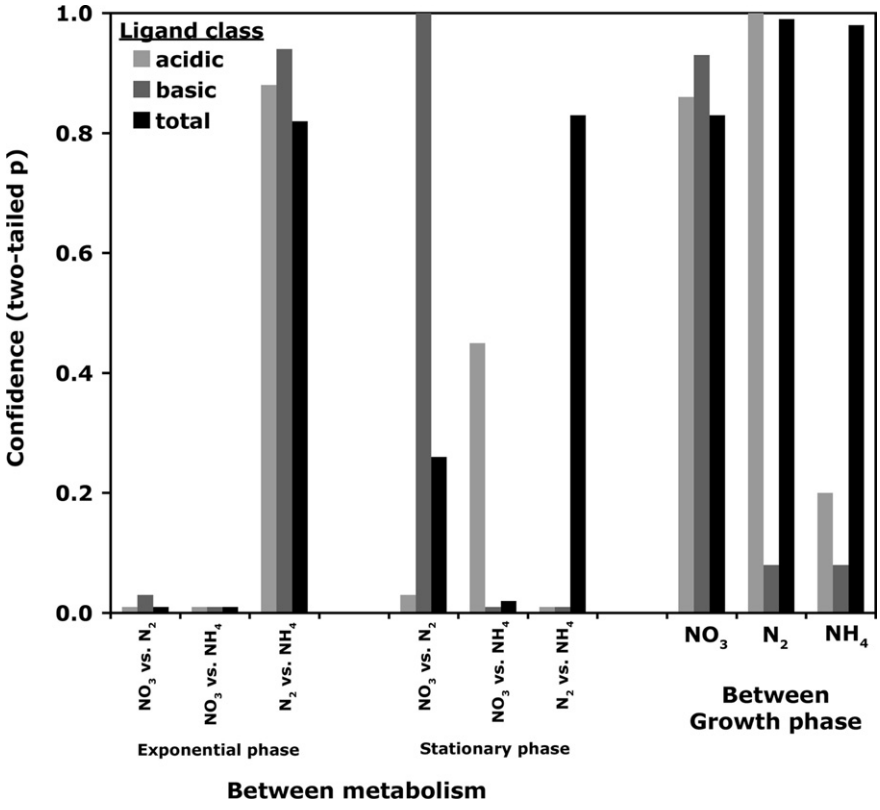

Fig. 4. Intervals of confidence in multiple pair-wise comparisons of ligand concentration, plotted as a function of comparison type: between-metabolism exponential phase comparisons (left), between-metabolism stationary phase comparisons (center), and between growth phase metabolism comparisons (right).

sess variability introduced as a consequence of batch culture conditions.

In order to ascertain the sources of variability, pair-wise probabilities were grouped according to metabolism and growth phase, and plotted in Fig. 4. It is evident that while confidence is generally poor in comparisons between cultures of different metabolism harvested at the same phase of growth, confidence in comparisons between growth phases of the same metabolism is higher (Fig. 4). The former is especially true for exponential phase cultures, where the greatest variability between metabolic treatments was observed; stationary phase cultures appeared less affected by different metabolic treatments. We conclude that for this organism, metabolic pathway is a greater determinant of ligand concentration than growth phase, as did Haas (2004) for *Shewanella putrefaciens*. It should be noted that variability in the distribution of ligands between acidic and basic pK_a values may result in largely unchanged total concentrations, as is the case between stationary and exponential ammonium-assimilating cells, as well as between stationary phase ammonium-assimilating and nitrogen fixing cells (Fig. 4). High confidence in comparisons of total ligand concentrations between ammonium-assimilating and nitrogen-fixing cultures simply indicates that they possesses similar overall reactivity summed over the titration range, despite possessing different distributions of individual ligands.

4. CONCLUSIONS

Ligand concentrations and pK_a distributions describing acid-base properties of the Gram-negative surface of the cyanobacterium *Anabaena* sp. strain PCC 7120 are reported and used to assess variability in surface chemistry as a function of batch culture growth conditions. It was determined that the observed variations in ligand concentration are not accurately accounted for using one set of parameters describing this bacterial surface. Future potentiometric evaluations of Gram-negative bacterial surface chemistry should benefit from the consideration of both growth phase and potential metabolic pathways. Furthermore, it was concluded that metabolic pathway was a greater determinant of ligand variability than growth phase. These results support the idea that, at least in the case of Gram-negative bacterial surfaces, the bacterial surface is a dynamic one where ligand distributions may evolve, for a single bacterial strain and over short (non-evolutionary) timescales, in response to nutritional or environmental demand.

REFERENCES

Baughman G. L. and Paris D. F. (1981) Microbial bioconcentration of organic pollutants from aquatic systems – a critical review. *Crit. Rev. Microbiol.* **8**, 205–228.

Beveridge T. J., Forsberg C. W. and Doyle R. J. (1982) Major sites of metal binding in Bacillus licheniformis walls. *J. Bacteriol.* **150**, 1438–1448.

Beveridge T. J. and Murray R. G. (1980) Sites of metal deposition in the cell wall of Bacillus subtilis. *J. Bacteriol.* **141**, 876–887.

Borrok D. and Fein J. B. (2005) The impact of ionic strength on the adsorption of protons, Pb, Cd, and Sr onto the surfaces of Gram negative bacteria: testing non-electrostatic, diffuse, and triple-layer models. *J. Colloid Interface Sci.* **286**, 110–126.

Borrok D., Fein J. B., Tischler M., O'Loughlin E., Meyer H., Liss M. and Kemner K. M. (2004) The Effect of Acidic Solutions and Growth Conditions on the Adsorptive Properties of Bacterial Surfaces. *Chem. Geol.* **209**, 107–109.

Brassard P., Kramer J. R. and Collins P. V. (1990) Binding site analysis using linear programming. *Environ. Sci. Tech.* **24**, 195–201.

Chamot D. and Owttrim G. W. (2000) Regulation of cold shock-induced RNA helicase gene expression in the cyanobacterium Anabaena sp. strain PCC 7120. *J. Bacteriol.* **182**, 1251–1256.

Chang J.-S., Law R. and Chang C.-C. (1997) Biosorption of lead, copper and cadmium by biomass of Pseudomonas aeruginosa PU21. *Wat. Res.* **31**, 1651–1658.

Claessens J., Behrends T. and Van Cappellen P. (2004) What do acid-base titrations of live bacteria tell us? A preliminary assessment. *Aquat. Sci.* **66**, 19–26.

Corapcioglu M. Y. and Kim S. (1995) Modeling facilitated contaminant transport by mobile bacteria. *Wat. Resour. Res.* **31**, 2648–2693.

Cox J. S., Smith D. S., Warren L. A. and Ferris F. G. (1999) Characterizing heterogeneous bacterial surface functional groups using discrete affinity spectra for proton binding. *Environ. Sci. Tech.* **33**, 4514–4521.

Daughney C. J. and Fein J. B. (1998) The effect of ionic strength on the adsorption of H^+, Cd^{2+}, Pb^{2+}, and Cu^{2+} by Bacillus subtilis and Bacilllus licheniformis: A surface complexation model. *J. Colloid Interface. Sci.* **198**, 53–77.

Daughney C. J., Fein J. B. and Yee N. (1998) A comparison of the thermodynamics of metal adsorption onto two common bacteria. *Chem. Geol.* **144**, 161–176.

Daughney C. J., Fowle D. A. and Fortin D. E. (2001) The effect of growth phase on proton and metal adsorption by Bacillus subtilis. *Geochim. Cosmochim. Acta* **65**, 1025–1035.

Fein J. B., Boily J. F. and Yee N. (2005) Potentiometric titrations of Bacillus subtilis cells to low pH and a comparison of modeling approaches. *Geochim. Cosmochim. Acta* **69**, 1123–1132.

Fein J. B., Daughney C. J., Yee N. and Davis T. A. (1997) A chemical equilibrium model for metal adsorption onto bacterial surfaces. *Geochim. Cosmochim. Acta* **61**, 3319–3328.

Fein J. B. and Delea D. E. (1999) Experimental study of the effect of EDTA on Cd adsorption by Bacillus subtilis: a test of the chemical equilibrium approach. *Chem. Geol.* **161**, 375–383.

Fortin, D., Ferris, F. G. and Beveridge, T. J. (1997) Surface-mediated mineral development by bacteria. In *Geomicrobiology: Interactions Between Microbes and Minerals* (eds. J. F. Banfield and K. H. Nealson), *Reviews in Mineralogy and Geochemistry 35*, Mineralogical Society of America, Washington, DC, pp. 161–180.

Fowle D. A. and Fein J. B. (1999) Competitive adsorption of metal cations onto two gram positive bacteria: testing the chemical equilibrium model. *Geochim. Cosmochim. Acta* **63**, 3059–3067.

Fowle D. A., Fein J. B. and Martin A. M. (2000) Experimental study of uranyl adsorption by *Bacillus subtilis*. *Environ. Sci. Tech.* **34**, 3737–3741.

Friis N. and Meyers-Keith P. (1986) Biosorption of uranium and lead by Streptomyces longwoodensis. *Biotech. Bioeng.* **28**, 21–28.

Haas J. R., Dichristina T. J. and Wade, Jr., R. (2001) Thermodynamics of U(VI) sorption onto Shewanella putrefaciens. *Chem. Geol.* **180**, 33–54.

Haas J. R. (2004) Effects of cultivation conditions on acid–base titration properties of *Shewanella putrefaciens*. *Chem. Geol.* **209**, 67–81.

Harris D. C. (1995) *Quantitative Chemical Analysis*. Freeman, New York, NY.

Hong Y. and Brown D. G. (2006) Cell surface acid–base properties of *Escherichia coli* and *Bacillus brevis* and variation as a function of growth phase, nitrogen source, and C:N ratio. *Coll. Surf. B* **50**, 112–119.

Hsu J. C. (1996) *Multiple Comparisons. Theory and Methods*. Chapman and Hall, London, England.

Kaneko T., Nakamura Y., Wolk C. P., Kuritz T., Sasamoto S., Watanabe A., Iriguchi M., Ishikawa A., Kawashima K., Kimura T., Kishida Y., Kohara M., Matsumoto M., Matsuno A., Muraki A., Nakazaki N., Shimpo S., Sugimoto M., Takazawa M., Yamada M., Yasuda M. and Tabata S. (2001) Complete genomic sequence of the filamentous nitrogen-fixing cyanobacterium *Anabaena* sp. strain PCC 7120. *DNA Res.* **8**, 205–213.

Konhauser K. O., Fyfe W. S., Ferris F. G. and Beveridge T. J. (1993) Metal sorption and precipitation by bacteria in two Amazonian river systems: Rio Solimoes and Rio Negro, Brazil. *Geology* **21**, 1103–1106.

Lindgvist R. and Enfield C. G. (1992) Cell density and non-equilibrium sorption effects on bacterial dispersal in ground water microcosms. *Microb. Ecol.* **24**, 25–41.

Lourenço S. O., Barbarino E., Lavin P. L., Lanfer Marquez U. M. and Aidar E. (2004) Distribution of intracellular nitrogen in marine microalgae: Calculation of nitrogen-to-protein conversion factors. *Eur. J. Phycol.* **39**, 17–32.

Madigan, M.T., Martinko, J.M. and Parker, J. (1997) Brock Biology of Microorganisms. 8th ed. Prentice Hall, Upper Saddle River, NJ.

Martinez R. E. and Ferris F. G. (2001) Chemical equilibrium modeling techniques for the analysis of high-resolution bacterial metal sorption data. *J. Colloid Interface Sci.* **243**, 73–80.

Martinez R. E., Smith D. S., Kulczycki E. and Ferris F. G. (2002) Determination of intrinsic bacterial surface acidity constants using a Donnan shell model and a continuous pK_a distribution method. *J. Colloid Interface Sci.* **253**, 130–139.

McCarthy J. F. and Zachara J. M. (1989) Subsurface transport of contaminants. *Environ. Sci. Tech.* **23**, 496–502.

Mérida A., Candau P. and Florencio F. J. (1991) Regulation of glutamine synthetase activity in the unicellular cyanobacterium *Synechocystis* sp. strain PCC 6803 by the nitrogen source: Effect of ammonium. *J. Bacteriol.* **173**, 4095–4100.

Ngwenya B. T., Sutherland I. W. and Kennedy L. (2003) Comparison of the acid-base behavior and metal adsorption characteristics of a Gram-negative bacterium with other strains. *App. Geochem.* **18**, 527–538.

Phoenix V. R., Martinez R. E., Konhauser K. O. and Ferris F. G. (2002) Characterization and implications of the cell surface reactivity of the cyanobacteria *Calothrix* sp. App.. *Environ. Microbiol* **68**, 4827–4834.

Plette C. C., Van Riemsdijk W. H., Benedetti M. F. and Van der Wal A. (1995) pH dependent charging behavior of isolated cell walls of a gram-positive soil bacterium. *J. Colloid Interface Sci.* **173**, 354–363.

Rinker K. D. and Kelly R. M. (2000) Effect of carbon and nitrogen sources on growth dynamics and exopolysaccharide production for the hyperthermophilic archaeon *Thermococcus litoralis* and bacterium *Thermotoga maritima*. *Biotechnol. Bioeng.* **69**, 537–547.

Rippka R., Deruelles J., Waterbury J. B., Herdman M. and Stanier R. Y. (1979) Generic assignments, strain histories and properties of pure cultures of cyanobacteria. *J. Gen. Microbiol.* **111**, 1–61.

Smith D. S., Adams N. W. H. and Kramer J. R. (1999) Resolving uncertainty in chemical speciation determinations. *Geochim. Cosmochim. Acta* **63**, 3337–3347.

Smith D. S. and Ferris F. G. (2001) Proton binding by hydrous ferric oxide and aluminum oxide surfaces interpreted using fully optimized continuous pK spectra. *Environ. Sci. Tech.* **35**, 4637–4642.

Smith D. S. and Kramer J. R. (1999) Multi-site proton interactions with natural organic matter. *Environ. Int.* **25**, 307–314.

Sokolov I., Smith D. S., Henderson G. S., Gorby Y. A. and Ferris F. G. (2001) Cell surface electrochemical heterogeneity of the Fe(III)-reducing bacteria *Shewanella putrefaciens*. *Environ. Sci. Technol.* **35**, 341–347.

Thormann K. M., Saville R. M., Shukla S. and Spromann A. M. (2005) Induction of rapid detachment in *Shewanella oneidensis* MR-1 biofilms. *J. Bacteriol.* **187**, 1014–1021.

van Loosdrecht M. C. M., Lyklema J., Norde W. and Zehnder A. J. B. (1989) Bacterial adhesion: A physicochemical approach. *Microb. Ecol.* **17**, 1–15.

van Loosdrecht M. C. M., Norde W., Lyklema J. and Zehnder A. J. B. (1990) Hydrophobic and electrostatic parameters in bacterial adhesion. *Aquat. Sci.* **52**, 103–114.

Wandersman C. and Delepelaire P. (2004) Bacterial iron sources: From siderophores to hemophores. *Ann. Rev. Microbiol.* **58**, 611–647.

Warren L. A. and Ferris F. G. (1998) Continuum between sorption and precipitation of Fe(III) on microbial surfaces. *Environ. Sci. Tech.* **32**, 2331–2337.

Wolk C. P. (1996) Heterocyst formation. *Annu. Rev. Genet.* **30**, 59–78.

Yee N., Fein J. B. and Daughney C. J. (2000) Experimental study of the pH, ionic strength, and reversibility behavior of bacteria-mineral adsorption. *Geochim. Cosmochim. Acta* **64**, 609–617.

Yee N., Fowle D. A. and Ferris F. G. (2004) A Donnan potential model for metal sorption onto *Bacillus subtilis*. *Geochim. Cosmochim. Acta* **68**, 3657–3664.

Associate editor: Lesley A. Warren